Electrochemical characterization of Na_xMO_2 as cathode materials in sodium battery

V.H. Nguyen*, M.L.P Le*, L.T.N. Huynh* and V.M. Tran**

*Applied Physical Chemistry Laboratory, VNUHCM-University of Sciences
227, Nguyen Van Cu street, Ho Chi Minh City, Vietnam, lmlphung@hcmus.edu.vn
**Department of Physical Chemistry, VNUHCM-University of Science
227, Nguyen Van Cu street, Ho Chi Minh City, Vietnam, tvman@hcmus.edu.vn

ABSTRACT

Na_xMO_2, with M = Mn and Co as cathode materials in sodium-ion batteries, was synthesized by solid-state reaction at 600–850°C. The manganese precusors were MnO_2 prepared from electrolysis of $MnSO_4$ solution, $MnCO_3$ and $Mn(AcO)_2$. The structure of synthesized materials was determined by X-rays diffraction and the morphology was investigated by Scanning Electron Microscope (SEM). The electrochemical properties were examined in 1M $NaClO_4$/PC as electrolyte by Cyclic voltagemetry (CV).The electrochemical behavior of synthesized materials exhibits complex insertion-deinsertion mechanism in the potential window 2 - 4 V vs Na^+/Na with multi-peak in CV curve. These peaks correspond to the phase transitions with inserted/deinserted sodium contents. $Na_{0.44}MO_2$ synthesized from manganese acetate compound exhibits well-crystallized rod-shape particle, highest capacity and good cycling behavior compared to other manganese sources.

Keywords: cathode materials, insertion-deinsertion mechanism, $Na_{0.44}NaO_2$, $Na_{0.74}CoO_2$, sodium-ion batteries.

1 INTRODUCTION

Since commercialization, Li-ion batteries have been playing an important role as power source for portable electronic devices because of high gravimetric, volumetric capacity and high voltage. Futhermore, Li-ion batteries have also been desired to be the large scale application such as hydrid electric vehicule or smart grid system; and thus, the demand of lithium raw material increases more and more. Unfortunately, the resource of lithium raw material is limited, increasing the price of these raw material. In order to solve the problem of lithium raw resoure, sodium is proposed as a solution for next generation power source storage, for example as sodium ion battery [1].

Some cathode materials in sodium ion battery were studied like layered metallic oxide or phosphorus oxide based transiton metals : Na_xMO_2, Na_xMPO_4 (M = Co, Ni, Mn, Ti…) which could intercalate sodium ion. Among them, $Na_{0.44}MnO_2$ and $Na_{0.74}CoO_2$ have been greatly attracted as a novel cathode material for sodium ion battery because of its theorical capacity of 121 mAh/g, 112 mA.h/g respectively and good performance [2].

For synthesis of $Na_{0.44}MnO_2$, solid state reaction is the first route with precusor of $MnCO_3$ and Na_2CO_3. Beside solid state reaction, $Na_{0.44}MnO_2$ was also prepared by polymer-pyrolysis method and hydrothermal route for nanostructure (nanowire, nanobelt) from CH_3COONa, $Mn(CH_3COO)_2$ [3-6]. The synthesis of $Na_{0.74}CoO_2$ was also reported by solid state reaction [7].

In this paper, we report the synthesis and electrochemical properties of Na_xMO_2 (M = Mn, Co) as cathode materials in sodium-ion battery. The Na_xMO_2 were prepared by different manganese source compounds such as: electrolytic MnO_2, $Mn(AcO)_2$ and $MnCO_3$.

2 EXPERIMENTALS

Na_xMO_2 materials with M = Mn and Co was prepared by solid-state reaction at 600-850°C. In case of manganese, the manganese precusors were MnO_2 obtained from electrolysis of $MnSO_4$ solution, $MnCO_3$ (Sigma Aldrich, 99,9%), $Mn(AcO)_2$ (Reagent ACS, > 99%), and Na_2CO_3 (Merck, > 99,9%). In case of cobalt, precusors were a mixture of $Co(NO_3)_2$ (Sigma Aldrich, 99,9%) and Na_2CO_3. All the precursors were heated at 300°C for 8 hours to decompose all of carbonates, acetate; then re-grounded and pressed into pellets. The pellets were calcinated repeatedly in air at diferent conditions (Table 1). After that, the final products were cooled to room temperature.

Table 1: Summary of Na_xMO_2 samples synthesized at different conditions.

Sample	Precusors		Temperature	Time
NMO-1	Na_2CO_3	$MnCO_3$	800°C	9 hours
NMO-2	Na_2CO_3	$Mn(AcO)_2$	800°C	9 hours
NMO-3	Na_2CO_3	MnO_2	800°C	9 hours
NCO-1	Na_2CO_3	$Co(NO_3)_2$	650°C	24 hours
NCO-2	Na_2CO_3	$Co(NO_3)_2$	800°C	24 hours
NCO-3	Na_2CO_3	$Co(NO_3)_2$	900°C	24 hours

Structures of these samples were identified by powder X-ray diffraction, using a X'Pert PRO MPD PANalytical diffractometer with Co Kα radiation, 0.02° and 20 s/step counting time. The diffraction patterns was collected for 2θ between 10° to 70°. The morphology and the distribution of grain size were determined by using a Carl Zeiss MERLIN Scanning Electronic Microscope (SEM) instrument.

The intercalation/deintercalation properties of Na_xMO_2 compounds were investigated by using Cycling voltammetry in organic electrolyte 1M $NaClO_4$/propylene carbonate. The electrochemical cell consits of three electrodes: the counter electrode was sodium wire, the reference electrode was sodium wire in $NaClO_4$ electrolyte, the working electrode was electrode material coated on the Au surface. The scaning rate used was 10 µV/s.

The cycling behavior of these materials were measured in a coin-type cell 2025. The positive electrode was composed on active material (80% wt.), acetylen black (7.5% wt.), graphite (7.5% wt.) and teflon (5% wt.). The mixture was pressed directly on a stainless steel grid under a pressure of 5 ton per cm^2. Negative electrode was sodium metal and $NaClO_4$ 1 M in propylene carbonate (PC) was used as electrolyte. Cells were assembled in a glove box under argon to avoid oxygen and water. Electrochemical studies were carried out by using VMP3 apparatus (BioLogic – France).

3 RESULTS AND DISCUSSION

3.1 $Na_{0.44}MnO_2$ material

$Na_{0.44}MnO_2$ crystallizes in an orthorhombic lattice cell with Pbam space group, which has large S-shaped tunnel structure. Structure of $Na_{0.44}MnO_2$ is built on square pyramides MnO_5 and octahera MnO_6 (Figure 1a). All Mn^{4+} ions and a half of Mn^{3+} ions are occupied in octaheral sites while other Mn^{3+} ions are located in square pyramids. In case of sodium ions, Na1 site is placed fully in the small tunnel while the Na2 and Na3 are situated a half in large S-shaped tunnels. According to this structure, direction of diffusion of sodium ions is oriented by axe c [8].

Table 2: Lattice parameters of $Na_{0.44}MnO_2$ samples

Sample	a (Å)	b (Å)	c (Å)	Cell volume (Å^3)
NMO-1	9.115	26.40	2.828	680
NMO-2	9.178	26.51	2.826	688
NMO-3	9.078	26.44	2.827	678

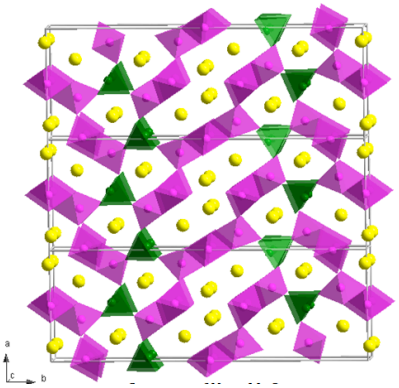

Figure 1a: Structure of $Na_{0.44}MnO_2$

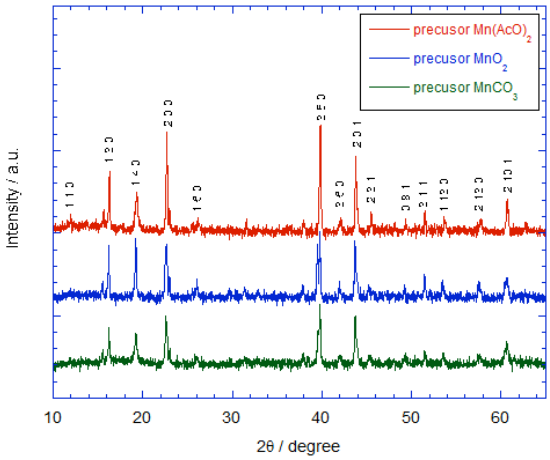

Figure 1b: XRD patterns of $Na_{0.44}MnO_2$ samples.

By using three different manganese sources, XRD patterns showed a well-crytallized $Na_{0.44}MnO_2$ orthorhombic phase (Pbam space group) without impurities. The lattice parameters were determined (Table 2), which are in good agreement with previous reports [5-6].

The morphology of $Na_{0.44}MnO_2$ samples was studied by scanning electron microscopy (SEM). The rod-shaped NMO particles are formed with typical dimensions of a few µm in length and about a 1 µm in width. The samples NMO-02 (precusor $Mn(AcO)_2$) exhibits well crytallized and homogenous rod-shape particles in comparison with NMO-01 and NMO-03.

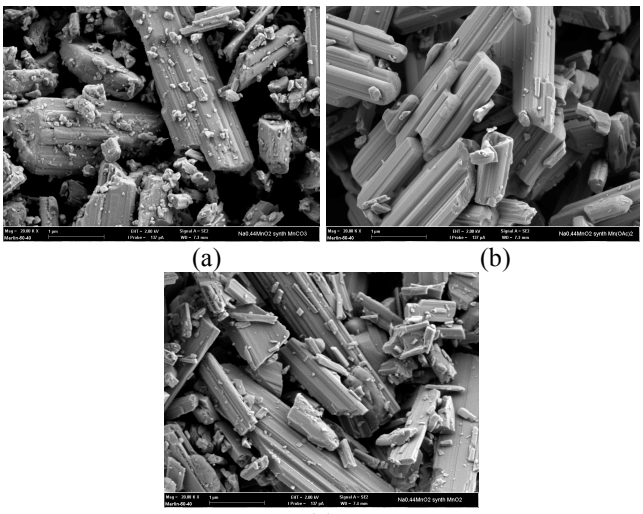

(a) (b)

(c)

Figure 2: SEM images of $Na_{0.44}MnO_2$ sample (a) NMO-01, (b) NMO-02, (c) NMO-03.

In Figure 3, CV curve of NMO-02 at a scan rate 10 µV/s presents 6 reversible redox pairs at anodic and cathodic scans, indicating the reversible complex insertion/deinsertion of Na ion into/out of the structure $Na_{0.44}MnO_2$ with a multiphase evolution. The sodium ion intercalated firstly in the site Na3 and Na2 (S-shaped tunnel), after that, sodium ion moved to the site Na1 (small tunnel) at the the end of intercalation. Sauvage *et al.* have reported that only 0.22 Na per unit can be extracted from

CTSI-Cleantech 2014, www.ct-si.org, ISBN 978-1-4822-5819-6

$Na_{0.44}MnO_2$, while 0.44 Na can be inserted back, resulting in evolution of Na concentration in the range of 0.22-0.66 [3].

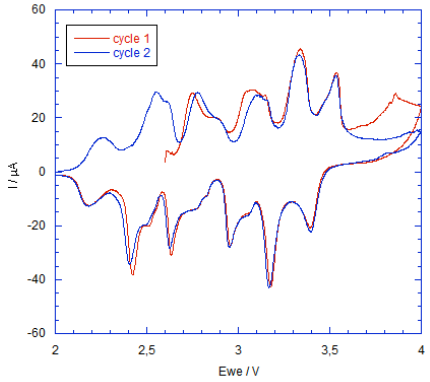

Figure 3: CV curve of NMO-02 at the scan rate 10 µV/s

In Figure 4a, the discharge curves of $Na_{0.44}MnO_2$ cathode materials in the potential range 2- 4 V vs Na^+/Na at C/10, shows the complex insertion/deinsertion mecanism of sodium ions. Six voltage plateaus are distinctly observed in the discharge curve, correspoding to 6 redox peaks in the CV curve. In the potential range of 2-4 V, the sample NMO-02 exhibits an initial capacity of 115 $mAh.g^{-1}$, about 95% of the theoretical one. The samples NMO-01 and NMO-03 present a capacity of 106 and 100 $mAh.g^{-1}$, respectively.

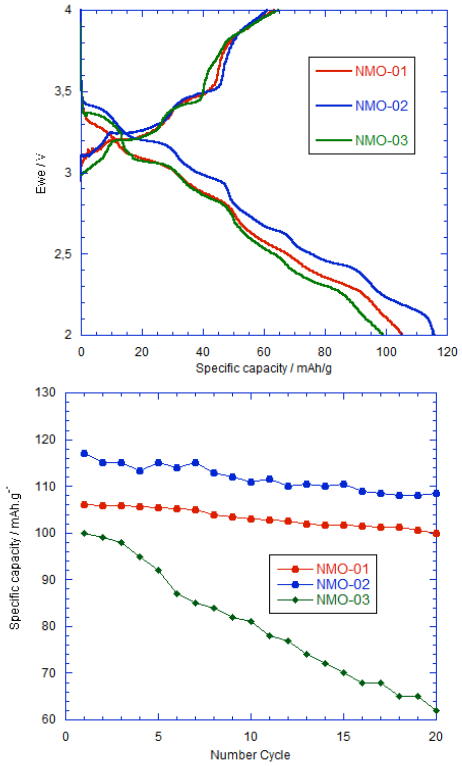

Figure 4: (a) 1st charge/discharge curve of Na_xMnO_2 and (b) Cycling performance of Na_xMnO_2 samples.

Figure 4b showed the cycling performance stability of $Na_{0.44}MnO_2$ at C/10. After 20 cycle, NMO-02 still has discharge capacity of 108 $mAh.g^{-1}$, maintain 90% of the initial value. NMO-01 is almost stable with a discharge capacity of 100 $mAh.g^{-1}$. However, capacity of NMO-03 is decreased afer each cycle, it presents a 62 $mAh.g^{-1}$ in 20th cycle. We believe that the capacity fading of NMO-03 which is affected by the morphology and the distribution of grain size. The homogeous particles morphology and well-crystallized grains facilitate the diffusion pathway of sodium ion in the small tunnel of $Na_{0.44}MnO_2$ [4].

3.2 $Na_{0.74}CoO_2$ material

$Na_{0.74}CoO_2$ crystallizes in a layer structure type P2-phase, which exhibits an ABBA oxygen packing with cobalt ions in octahedral sites and sodium ions in two different types of trigonal prismatic site: Na_f shares only faces with two CoO_6 octahedra of adjacent slabs, whereas Na_e shares edges with the six surrounding CoO_6 octahedra [7,9].

Figure 4b shows the XRD patterns of $Na_{0.74}CoO_2$ materials synthesized at different temperatures. The XRD peaks could be assigned to the reflection of crystal structure type of P2-phasewwith spacegroup P63/mmc. All three samples synthesized at 650°C, 800°C, 900°C during 24h, the lattice parameters are found to be in the range a = 2.83 Å and c = 10.88 Å which are in good agreement with the previous reports. Moreover, the phase P2-$Na_{0.74}CoO_2$ appeared clearly at the beginning of 650°C instead of the presence of Co_3O_4 impurities. The samples at 800°C and 900°C exhibit single P2-phase without impurities.

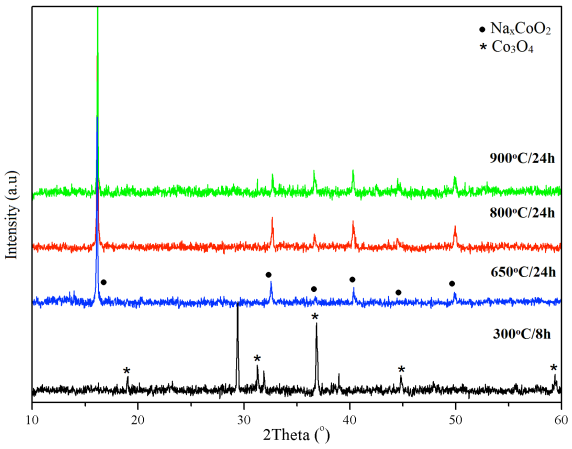

Figure 5: XRD patterns of $Na_{0.74}CoO_2$ samples.

The electrochemical performance of $Na_{0.74}CoO_2$ materials was showed in Figure 5. This material could intercalate 0.45 ion sodium in the structure for the Na content per formula about $0.5 < x < 1$. As previous reported, Na intercalation and deintercalation cycled between 2.0 – 3.8V undergoes complicated series of successively phase transitions, which have been investigated by in-situ XRD measurement [10]. The charge/discharge curve of P2-phase $Na_{0.74}CoO_2/NaClO_4/Na$ cell exhibits different small voltage domains with narrow sodium composition range, particularly 4 plateaux principal

at 3.6, 3.2, 2.9 and 2.6 V (Figure 5). The initial charge and discharge are found to be about 60 and 90 mAh.g^{-1}.

The cycling performance of $Na_{0.74}CoO_2$ was presented in Figure 6. The discharge capacity in the 20th cycle is 97%, which is 97% of the initial value. The retention capacity may be better in $NaPF_6$ electrolyte than in $NaClO_4$ electrolyte, as reported previous by Tirado's group [11].

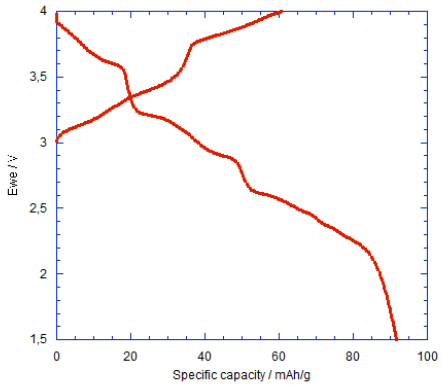

Figure 5: 1st charge/discharge curve of $Na_{0.74}CoO_2/NaClO_4/Na$ cell.

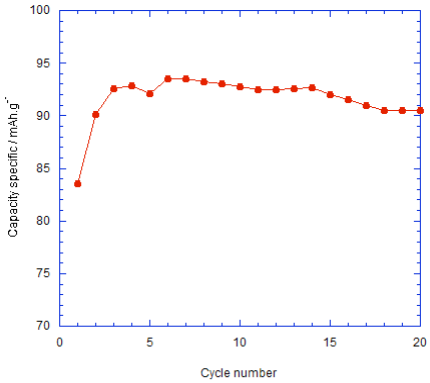

Figure 6: Cycling performance of $Na_{0.74}CoO_2/NaClO_4/Na$ cell.

4 CONCLUSIONS

In this work, the cathode materials were sucessfully synthesized by a solid state reaction in air. $Na_{0.44}MnO_2$ prepared from precusor $Mn(AcO)_2$ exhibit a well-crystallized, highest capacity (115 mAh.g^{-1}) and besy cycling performance compared to other precursors. The $Na_{0.74}CoO_2$ material showed a capacity of 93 mAh.g^{-1} and good cyclability. Further work is needed to explore the multiphase transition of $Na_{0.44}MnO_2$ during the charge/discharge process.

ACKNOWLEDGEMENTS

This work was supported by Vietnam National University of Ho Chi Minh City throught grant B2011-18-01-TĐ. We would like to thank the support of Group GESMAT (ICMPE – UMR 7182, France)

REFERENCES

[1] Palomares V., Serras P., Villaluenga I., Hueso K. B., Carretero-Gonzalez J. and Rojo T, Energy Environ. Sci., 5, 5884–5901, 2012.
[2] Slater M. D., Kim D., Lee E. and Johnson C. S., Adv. Funct.Mater., 23(8), 947-958, 2012.
[3] Sauvage F., Laffont F., Tarascon J-M. and Baudrin E, Inorg. Chem., 48(8), 3289 – 3294, 2007.
[4] Honoso E., Saito T., Okubo M., Saito Y., Nishio-Haname D., Kudo T. and Zhou H., Journal of Power Source, 217, 43-46, 2012
[5] Zhao L., Ni J. F., Wang H. and Gao L. J, Funct. Mater. Lett. 6(2), 1350012-1350016, 2013
[6] Zhao L., Ni J., Wang. and Gao L., RCS Advances, 3(18), 6650-6655, 2013
[7] Berthelot R., Carlier D. and Delmas C., Nat. Mat., 10(1), 74-80, 2010
[8] Kim H.J., Kim D.J., Seo D.H., Yoem M.S., Kang K.S., Kim D.K. and Jung Y.S., Chem. Mat. 24(6), 1205-1211, 2012
[9] Ding J. J., Zhou Y. N. and Sun Q., Electrochim. Acta 87, 388-393, 2013
[10] R. Berthelot, D. Carlier, C. Delmas, Nature Materials 10, 74, 2011.
[11] C. Vidal-Abarca, P. Lavela, J. L. Tirado, A.V. Chadwick, M. Alfredsson, E. Kelder, Journal of Power Sources 197, 314, 2012.